Co-published by
Institute of Fluid-Flow Machinery
Polish Academy of Sciences
Committee on Thermodynamics and Combustion
Polish Academy of Sciences

http://www.imp.gda.pl/archives-of-thermodynamics/

Comparative Analysis of Cylinder-to-Cylinder Variation of Parameters of an Automotive CRDI Engine

Saravanan Subramani[a*], Paul Durai Kumar[b], Ravi Govindasamy[b], Meenakshi Sundaram Iyamperumal[c]

[a]Department of Mechanical Engineering, Sri Venkateswara College of Engineering, Chennai 602117, Tamil Nadu, India
[b]Department of Automobile Engineering, Sri Venkateswara College of Engineering, Chennai 602117, Tamil Nadu, India
[c]Chief Technology Officer – M/S Amalgamations Component Division, Chennai, India
[*]Corresponding author e-mail: saran@svce.ac.in

Received: 07.05.2025; revised: 09.09.2025; accepted: 12.09.2025

Abstract

In the present work, an automotive three cylinder compression ignition engine employed with a common rail direct injection system, fuelled with diesel was investigated to analyse its performance and emission characteristics, and also cylinder-to-cylinder variation of important parameters of combustion. Variation of cylinder pressure, peak cycle pressure, rate of maximum pressure rise, rate of maximum heat release and combustion duration between the cylinders was presented as a function of brake mean effective pressure, torque and speed of the engine. Variation of carbon monoxide, unburnt hydrocarbon, oxides of nitrogen and brake thermal efficiency for the tested engine was presented as a function of brake mean effective pressure. It can be seen that measured combustion parameters show a significant variation between the cylinders, and the variation of the magnitude of average cylinder pressure was marginal. The peak pressure and combustion duration in cylinder 2 are higher by approx. 11% and 9%, respectively, than those of the other two cylinders. At a 40 Nm torque and at the lowest operated speed, the peak pressure in cylinder 2 is higher by 10% than that of the other two cylinders. This trend was also observed at the highest operated speed, with the peak pressure higher by approx. 14%. The maximum combustion duration in cylinder 2 was observed to be 9% higher than in the other two cylinders at identical comparable brake mean effective pressure values. It can also be seen that emission parameters were varied considerably with brake mean effective pressure and a trade-off point was obtained between NO_x-CO, NO_x-UBHC and NO_x-BTE.

Keywords: Common rail direct injection; Cylinder to cylinder; Emission; Combustion; Torque; Speed

Vol. 46(2025), No. 4, 105–115; doi: 10.24425/ather.2025.156841

Cite this manuscript as: Subramani, S., Kumar, P.D., Govindasamy, R., & Iyamperumal, M.S. (2025). Comparative Analysis of Cylinder-to-Cylinder Variation of Parameters of an Automotive CRDI Engine. *Archives of Thermodynamics*, 46(4), 105−115.

1. Introduction

Compression ignition (CI) engines are very common in medium and heavy duty automotive vehicles due to their high thermal efficiency, durability and robustness in nature. In a conventional direct injection (DI) multi-cylinder CI engine, it is very difficult to attain identical combustion in all the engine cylinders. Engine performance and emission with respect to speed and load are hampered by uneven combustion performance of the worst cylinders, which leads to misfiring and too early combustion phasing. The temperature of the inlet air, fuel supply, fuel injection timing, injection delay, ignition delay, air-fuel ratio, compression ratio, port geometry, gas exchange, exhaust gas recirculation supply, and cylinder cooling are the most important factors which can differ from cylinder to cylinder. The difference in any or in combinations of these factors is responsible for load variations and combustion phasing between the cylinders, which in turn may lead to power loss, increased mechanical vibration, cylinder-to-cylinder torque imbalance and engine emissions [1−3].

Nomenclature

CA – crank angle, °
p – pressure, bar
S – estimated factor (governed by different self-governing variables)
x_1, x_2, x_3, …, x_n – variables

Abbreviations and Acronyms

BMEP– brake mean effective pressure
BTE – brake thermal efficiency
CD – combustion duration
CI – compression ignition
CO – carbon monoxide
CRDI– common rail direct injection (system)
DI – direct injection
ECU – electronic control unit
MHRR– maximum heat release rate
MROPR– maximum rate of pressure rise
NO_x – oxides of nitrogen
SOC – start of combustion
TDC – top dead centre
UBHC– unburnt hydrocarbon

To save the environment and to improve the fuel economy, very stringent emission norms were developed, which cannot be attained by a conventional mechanical fuel injection system. This paved the way for the development of a high pressure injection system called common rail direct injection (CRDI) system [4,5]. In modern CI engines, an accumulator, simply called as common rail, is the main component in the CRDI system, which accumulates the fuel at high pressure in the range of 1000 bar to 2000 bar, and the fuel is injected into the cylinders through the respective fuel injectors. Injecting the fuel at higher pressure makes the fuel droplets to travel a longer distance inside the cylinder by penetrating the hot compressed air, and also atomises the fuel droplets into very fine particles. These two factors make the fuel vaporise at a much faster rate, which thereby improves the fuel-air mixing, and in turn leads to better combustion characteristics. In the CRDI system, by regulating the accumulator pressure, the fuel injection pressure can be controlled.

Since the fuel injection in the CRDI system is monitored by an electronic control unit (ECU), the required fuel quantity can be supplied at an exact time by either a single injection or multiple injections. Injecting a small quantity of fuel in advance and a subsequent injection to the regular injection refers to as a pilot and post injection, respectively. Pilot injection reduces the combustion noise by the gradual progress of combustion reactions in the cylinder [6,7]. The residence time of the pilot injected fuel's vapour phase will be comparatively longer, which allows the proper mixing with the air trapped in the cylinder. The pilot injected fuel burns after undergoing the pre-combustion reactions, resulting in greater cylinder temperature, so that the primary injected fuel begins to combust after causing a short delay period. This results in a reduced maximum rate at which the pressure increases, resulting in lower combustion noise. Hence, an overwhelming interest was created among the researchers and scientists to investigate the combustion features of the CRDI engine.

Cyclic and cylinder variations can be effectively controlled by suitably adjusting the injection timing and amount of exhaust gas recirculation (EGR). Many researchers have analysed the diesel engine characteristics with diesel and its alternatives [8−13]. Attempts were made on a single cylinder CI engine with different vegetable oils like karanja [14], jatropha [15], sunflower [16], cottonseed [17], rape seed [18], palm [19], rice bran [20], corn [21] and neem [22] in their blended forms with diesel and also in the converted forms of biodiesel.

It was inferred that vegetable oils in their pure forms and their derivatives have the capability to be used as a partial replacement of diesel in CI engines without any engine modifications, and the performance characteristics were comparable with those of diesel.

Attempts were also made to explore the outcome of changing engine design considerations on the engine characteristics with diesel and its alternatives [23−25]. In all these investigations, a single cylinder stationary engine [26−29] or an automotive engine employing mechanical fuel injection [30−35] was utilised. The CRDI concept was also attempted on a one cylinder stationary CI engine by increasing the fuel injection pressure [36−39]. Investigations have been carried out by modifying a single cylinder engine with the CRDI setup [38,39].

In all earlier research on the CRDI diesel engine, the concept of injecting fuel at a relatively higher pressure than the conventional injection pressure was attempted [36−45] and an actual automotive engine was not tested to analyse its performance, emission and combustion characteristics. Investigations carried out with automotive engines were also restricted to constant speed, and fuel injection characteristics were not controlled by ECU. To understand the behaviour of the CRDI engine, it is necessary to test a real time automotive engine to analyse its characteristics. In the earlier work, the authors have compared the combustion characteristics of an automotive CRDI engine with a conventional high-power compression ignition (HCV) engine through the measurement of combustion parameters in the first cylinder of the engine [46].

After analysing a wide range of literature, a certain gap was observed in the area of CRDI engine where the investigations of variations among cylinders of an automotive CRDI engine were not sufficiently addressed in the previous research works. Most of the reported works on multi-cylinder engines were restricted to investigate the characteristics of the engines through the measurement of combustion parameters of one of the cylinders.

Hence, to overcome these limitations, an attempt was made on an automotive passenger car CRDI engine to study the variation of combustion characteristics among the cylinders by measuring the cylinder pressure of all three cylinders using a separate pressure transducer for individual cylinders. The attempt was also extended to study the performance and emission characteristics of the engine at different operating conditions. The key objectives of this investigation are outlined as:

– to analyse the cylinder-to-cylinder variation of different combustion parameters of an automotive CRDI engine by operating the engine at different speeds and torque values,

– to investigate the performance and emission characteristics of an automotive CRDI engine with respect to different brake mean effective pressures (BMEP).

2. Experimental methodology

2.1. Experimental setup

An automotive, four stroke, three cylinder CRDI diesel engine manufactured for use in a passenger car was tested in the present investigation. Table 1 shows the details of the three cylinder engine used for testing, and the line diagram seen in Fig. 1 displays the setup used to conduct the experiments.

Table 1. Specifications of engine.

Arrangement	**Inline, 3 cylinder**
Volume (l)	0.98
Bore x stroke (mm)	73 x 78
Rated power (kW)	40 kW @ 4000 rpm
Peak torque (Nm)	130 Nm @ 1750–2750 rpm
Fuel system	unit pump common rail, 1600 bar system
Engine aspiration	turbocharged and cooled

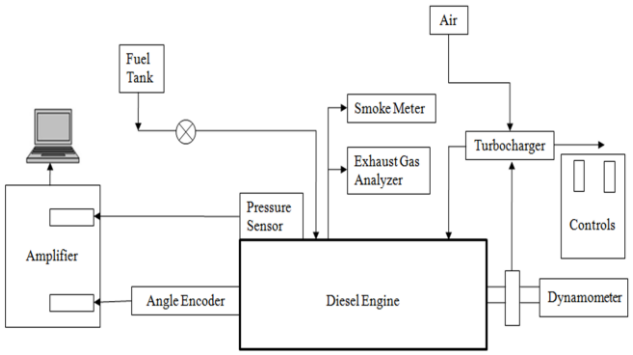

Fig. 1. Layout of experimental setup.

A dry gas type eddy current dynamometer ECB-120 HP was attached to the test engine as a loading device. Each of the three cylinders is fitted with a separate pressure transducer to record the pressure generated inside the individual cylinder and instrumented with an angle encoder to note down the pressure inside the cylinder at various crank angles. The pressure signals were amplified by their respective charge amplifier and then fed to an AVL data acquisition system to interpret the recorded in-cylinder pressure and stored in a personal computer. An AVL exhaust gas analyser and AVL smoke meter were employed in engine emission measurements. Table 2 shows the range, accuracy and percentage uncertainties of the instruments used for emission measurement.

2.2. Test conditions

As per the standards of the modified Indian duty cycle, the small sized passenger cars were allowed to operate around 50 per cent of the maximum rated speed and torque to simulate the normal driving conditions and further lower range for city driving conditions. Hence, the test conditions of the engine were selected to represent the same. The test matrix selected for the investigation is shown in Table 3, and Table 4 shows the properties of diesel.

Table 2. Range, accuracy and percentage uncertainties of instruments.

Instrument	Measured quantity	Range	Accuracy	Uncertainties, %
AVL DIGAS 444 Exhaust gas analyzer	NO_x	0–5000 ppm	±10 ppm	0.2
	UBHC	0–20000 ppm n-hexane	±50 ppm	
	CO	0–20%	±5%	
AVL 437C Smoke meter	Smoke opacity	0–100 %	±2 %	1.0

Table 3. Test matrix.

S. No.	Speed (rpm)	Torque (Nm)
1	1850	65
2	2000	30
3	1550	40
4	1300	45
5	1850	50
6	1000	55
7	1250	60
8	1750	65
9	1050	40
10	1100	40
11	1250	40
12	2000	40
13	1250	30
14	1250	45
15	1250	50
16	1250	60

Table 4. Properties of diesel [46].

Property of fuel	Method	Diesel
Viscosity at 40°C (mm^2/sec)	ASTM D445	3.522
Flash point (°C)	ASTM D93	70
Calorific value (kJ/kg)	ASTM D240	43000
Distillation temperature T90 (°C)	ASTM D86	335
Specific gravity	ASTM D4052	0.8

To explore the deviation of combustion parameters as an element of BMEP, the engine was tested at different operating conditions by varying both the engine speed and torque as specified in Table 3. To investigate the effect of speed and torque on combustion parameters, tests were conducted by maintaining the engine torque at 40 Nm for different speeds and also by changing the torque at a uniform speed of 1250 rpm as shown in Table 3.

2.3. Test procedure

In order to stabilise the engine operating conditions, the test engine was operated for a short span of time at idle speed with no

load condition. After the engine was stabilised, it was operated at different operating conditions as specified in the test matrix given in Table 3. The test engine was also made to run at different speeds by maintaining a steady torque of 40 Nm and dissimilar torques by retaining an identical speed of 1250 rpm. At each operating condition, performance, emission and combustion parameters were documented and analysed.

2.4. Uncertainty analysis

The errors linked with the measurements of different combustion parameters were calculated. The maximum potential errors in the measurement of pressure and crank angle were predicted by employing the technique recommended by Moffat [47]. From the least measured values and the measuring instrument's accuracy, the possible errors were calculated.

If an estimated quantity S depends on multiple independent variables (x_1, x_2, x_3, …, x_n), the associated error in S can be expressed as shown in Eq. (1):

$$\frac{\partial S}{S} = \left\{\left(\frac{\partial x_1}{x_1}\right)^2 + \left(\frac{\partial x_2}{x_2}\right)^2 + \ldots\ldots\ldots\ldots + \left(\frac{\partial x_n}{x_n}\right)^2\right\}^{\frac{1}{2}}, \quad (1)$$

where ($\partial x_1/x_1$), ($\partial x_2/x_2$), etc. are the errors in the independent variables, ∂x_1 depicts the accuracy of the measuring instrument, and x_1 depicts the least measured output value.

2.4.1. Calculation of errors in measured parameters

The pressure inside the combustion chamber was measured by commissioning a pressure transducer, and the electrical signal received was amplified with the help of a charge amplifier. The crank angle degree was measured with the help of a crank angle encoder. The accuracy of the pressure measurement instrument employed is 0.01, and that of the crank angle measurement is 0.02. Hence, the values of maximum possible errors for pressure and crank angle measurements are calculated as shown below:

Cylinder pressure

The minimum value of cylinder pressure measured while conducting the investigations is 0.72 bar with an accuracy of 0.01. Therefore, the maximum possible error during the measurement of pressure is calculated using Eq. (2):

$$\left(\frac{\partial p}{p}\right)_{EXP} = \left(\left(\frac{0.01}{0.72}\right)^2\right)^{\frac{1}{2}} \cdot 100 = 1.38\%. \quad (2)$$

Crank angle

The minimum degree of measured crank angle during the experimentation is 1 degree, and the measurement accuracy is 0.02. Therefore, the calculated maximum possible error in the measurement of crank angle is calculated using Eq. (3):

$$\left(\frac{\partial CA}{CA}\right)_{EXP} = \left(\frac{0.02}{1}\right) \cdot 100 = 2\%. \quad (3)$$

3. Results and discussion

3.1. Cylinder pressure and heat release rate

Figures 2 and 3, respectively, display the deviation of pressure inside the cylinder and the variation of heat release rate for all the three cylinders of the test engine based on crank angle degree (º*CA*) for a total range of 60º*CA* (−30º*CA* to 30º*CA* with respect to top dead centre (TDC) position) for an operating speed of 1850 rpm and torque 65 Nm.

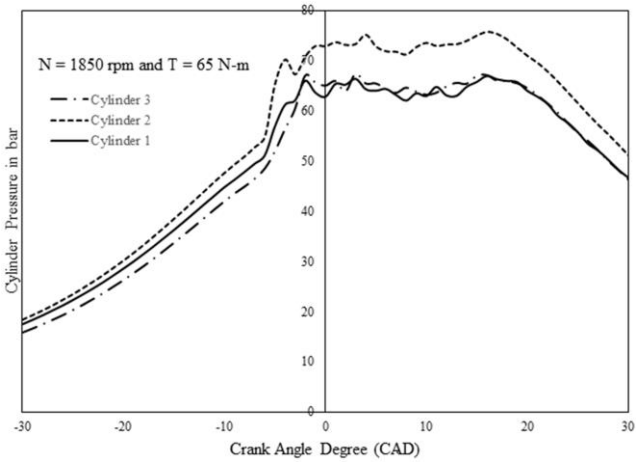

Fig. 2. Variation of cylinder pressure.

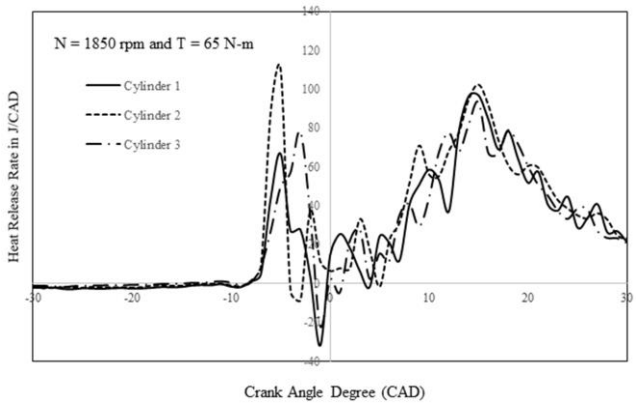

Fig. 3. Variation of heat release rate.

From Fig. 2, it can be perceived that the magnitude of cylinder pressure increases steadily for all three cylinders as the piston moves towards TDC, and the pressure of cylinder 1 lies between those of cylinder 2 and cylinder 3. Until the piston reaches 6º*CA* before TDC (bTDC), the variation in pressure between cylinder 1 and cylinder 2 is marginal (cylinder 1 has a higher value), and the variation in pressure between cylinder 1 and cylinder 3 is also around 3 bar (cylinder 3 has a higher value). At 5º*CA* bTDC, the pressure in cylinder 2 increases steeply, and its variation with other cylinders increases, and almost the same difference is maintained throughout the remaining cycle as shown in Fig. 2. This may be attributed to the marginal variation of the injected fuel quantity and its compression, which may result in a higher pressure for cylinder 2 when compared with the

other cylinders. It was also observed that the peak pressure for all three cylinders occurred at 16º*CA* after TDC (aTDC).

From Fig. 2, it can also be seen that after the completion of ignition delay, in-cylinder pressure variation between the different phases of combustion was marginal. It can also be seen that the difference between the magnitude of average cylinder pressure (measured during the uncontrolled and controlled combustion phase) and peak pressure was also marginal. This may be due to the influence of pilot fuel injection employed in the test engine. As the injection is carried out in two phases as pilot injection and main injection, the peak pressure is occurred at two positions, one bTDC due to pilot injection and the other aTDC due to main injection and the former was lower than the latter. This may be due to the fact that more fuel was injected through the main injection when compared with that of the pilot injection, and the injected fuel will be burned immediately after entering the combustion space, which leads to a larger peak pressure aTDC. Higher pressure of fuel injection in the test engine enhances the fuel atomisation and vaporisation by providing smaller fuel particles, which in turn improves the combustion process. This results in smooth combustion during pilot and main injections, which leads to a marginal variation in pressure during the combustion.

From Fig. 3, it can be witnessed that after the completion of the delay period, the rate of heat release for all cylinders was higher due to the combustion of the accumulated charge through pilot injection. The maximum heat release due to pilot injection was obtained at 5º*CA* bTDC for cylinder 1 and cylinder 2, and at 3º*CA* bTDC for cylinder 3 whose magnitude of heat release lies between that of cylinder 1 and cylinder 2. The maximum heat released at this condition was obtained in cylinder 2. This may also be due to the increased charge pressure as a result of a marginal increase in compression of injected fuel, which may improve the combustion and, in turn, increase the combustion temperature. Likewise, the heat release rate increased in the course of the expansion stroke, and the maximum heat release obtained in all three cylinders occurred at 15º*CA* aTDC, the value for cylinder 2 being the highest and the value for cylinder 1 lying between those of cylinder 3 and cylinder 2. As discussed earlier, the volume of the main injected fuel is larger, which leads to a greater heat release rate than that obtained during the pilot injection period. A negative heat release rate is also observed at a location close to that of TDC (bTDC). This is due to the delay in the start of combustion of injected fuel during the primary injection, which absorbed the heat generated due to combustion of the pilot injection.

3.2. Combustion parameters as a function of BMEP

In this section, the variation of different combustion parameters is presented as a function of BMEP. Torque and speed of the engine given in Table 3 were chosen to represent the combustion parameters as a function of BMEP. The characteristics of the pilot injection and main injection at different operating conditions employed in the engine are depicted in Table 5.

Injecting a small portion of fuel as pilot injection will drastically reduce the combustion noise, combustion temperature, and thereby reduce the formation of nitrogen oxides. Table 5 clearly shows that 10 per cent of the fuel was injected through pilot injection and the remaining 90 per cent of fuel was injected through main injection. It also shows that the start of pilot injection occurred between 7.5º*CA* bTDC and 10º*CA* bTDC, and the main injection occurred very close to TDC. The fuel injection timing and quantity vary as the engine operates at different speeds and torques, which is also presented in Table 5.

Table 5. Characteristics of pilot injection and main injection.

Speed (rpm)	Torque (Nm)	Pilot injection			Main injection		
		Start of Injection	Fuel (mg/str.)	Inj. pulse duration (µs)	Start of Injection	Fuel (mg/str.)	Inj. pulse duration (µs)
2000	30	-8.2	0.682	29	1.74	6.827	287
1550	40	-9.05	0.797	35	1.01	7.972	345
1300	45	-9.3	0.954	42	0.76	9.542	415
1850	50	-7.8	1.065	39	2.3	10.65	387
1000	55	-9.32	1.216	52	0.69	12.17	524
1250	60	-9.3	1.190	46	0.69	11.91	463
1750	65	-8.02	1.296	43	1.88	12.96	432
1050	40	-9.2	0.769	39	0.69	7.696	386
1100	40	-9.2	0.780	38	0.69	7.801	384
1250	40	-9.3	0.811	38	0.69	8.116	381
2000	40	-7.5	0.905	35	2.54	9.058	347
1250	30	-10	0.539	28	0.03	5.391	279
1250	45	-9.2	0.979	43	0.69	9.795	430
1250	50	-0.93	1.167	48	0.69	11.67	484
1250	60	-9.2	1.422	54	0.69	14.22	538

The variation of peak pressure is shown in Fig. 4(a) as a function of BMEP for all three cylinders. It is found that the peak pressure for all cylinders increases with an increase in BMEP. This might be the effect of increased volume of charge burned, releasing more heat, which in turn increases the cylinder pressure and therefore results in a higher peak pressure as BMEP increases. Engine operation was also found to be smoother for all three cylinders as a result of the peak pressure varying almost linearly with BMEP.

Variation of the maximum rate of pressure rise (MROPR) as a function of BMEP is shown in Fig. 4(b). It is observed that the rate of pressure rise shows an erratic trend with BMEP. As the start of combustion is advanced with BMEP, the delay period will be shorter, resulting in lower MROPR at higher BMEP. An increase in MROPR with BMEP may be due to the change in the start of combustion with BMEP.

Figure 4(c) displays the manner in which the start of combustion (SOC) varies with BMEP for cylinder 1, cylinder 2 and cylinder 3. It is observed that with an increase in BMEP, SOC advances. The earlier SOC at a higher BMEP may be due to an increase in the fuel quantity burned and combustion chamber temperature, which in turn enriches fuel vaporisation and shortens the ignition delay period as BMEP increases. The same trend is observed for all three cylinders. It is also seen that at lower BMEP, SOC of cylinder 2 lies between those of cylinder 1 and

cylinder 3, but as BMEP increases, SOC of cylinder 2 is slightly advanced than for the other two cylinders. A delay in SOC is also observed at a higher BMEP for all three cylinders. This may be due to the change in the pilot injection period with respect to the engine operating conditions.

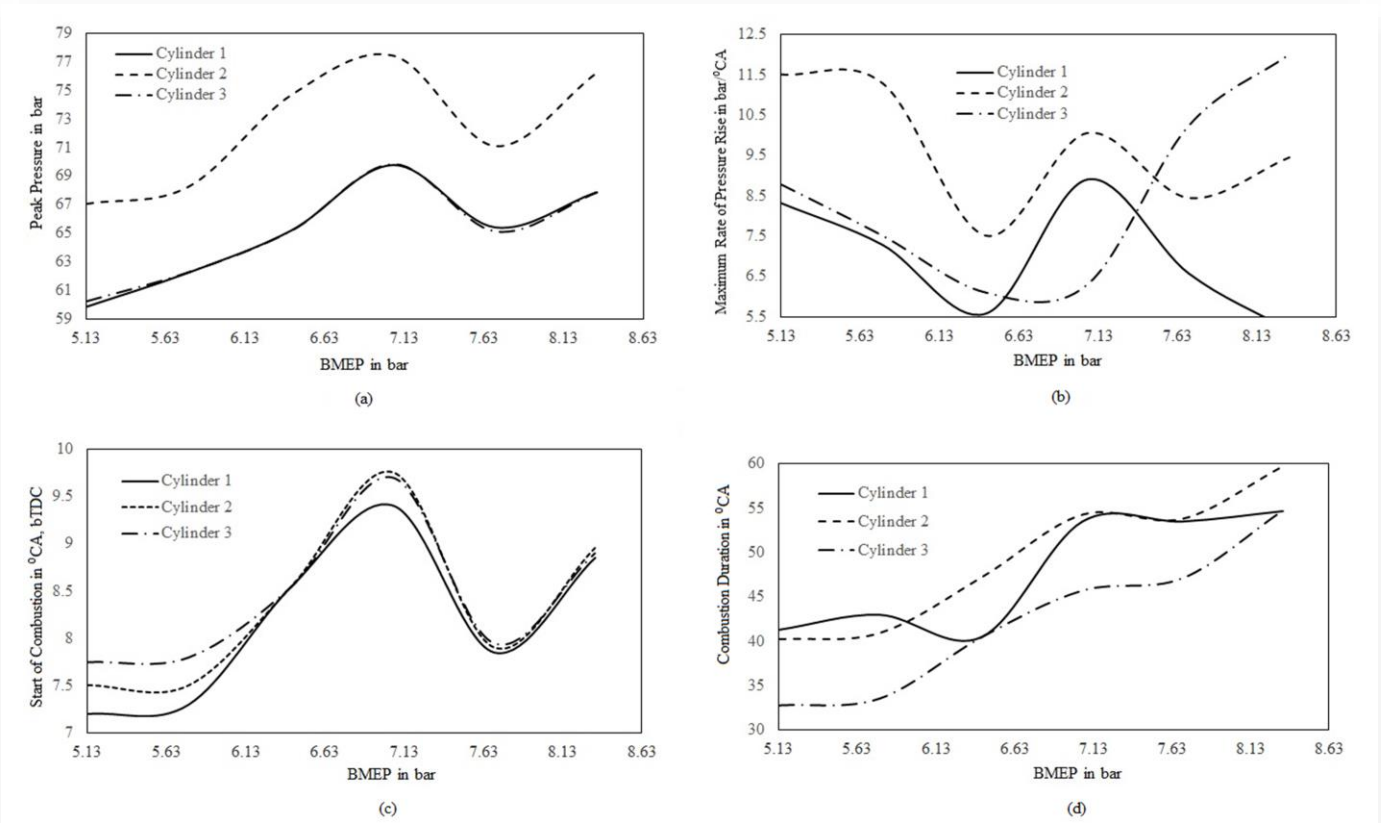

Fig. 4. Variation of combustion parameters with BMEP.

Figure 4(d) displays the deviation of combustion duration (CD) with respect to BMEP. It is inferred that an increase in the value of BMEP escalates CD. Cylinder 2 and cylinder 3 show a similar trend, and cylinder 2 shows a marginally longer CD than the other cylinders. This may be the effect of injecting a higher volume of fuel as BMEP is increased, which in turn may increase the period of fuel burning. Cylinder1 deviates from the other two cylinders, showing an erratic trend.

3.3. Influence of speed and torque on combustion parameters

The influence of engine speed and torque on engine combustion parameters like SOC, CD, peak cylinder pressure, maximum heat release rate 1 (MHRR1) due to secondary injection, maximum heat release rate 2 (MHRR2) due to main injection and maximum rate of pressure rise (MROPR) are presented and discussed in this chapter. The combustion parameters are recorded and investigated at two different engine running conditions:

(a) different torques at a uniform speed, 1250 rpm,
(b) different speeds at a uniform torque, 40 Nm.

3.3.1. Influence of speed on combustion parameters

Here, the variation of combustion features as a function of speed for all three cylinders is presented and discussed. It is observed in Fig. 5(a) that the cylinder peak pressure is less affected for the individual cylinders when the engine is operated at different speeds by maintaining a constant torque, but the peak pressure of cylinder 2 is marginally higher than those of cylinder 1 and cylinder 3. From Fig. 5(b), it is observed that MROPR is increased with respect to speed till it attains its maximum value and after that, MROPR is found to be decreased at higher speeds. The same trend is followed for all three cylinders, but for cylinder 2, MROPR at lower speeds is much higher than for the other cylinders.

Figure 5(c) shows that as the engine speed increases, SOC is slightly advanced in order to provide adequate time for complete combustion. This may be due to the fact that the combustion duration remains the same in terms of milliseconds, but it slightly increases in terms of crank angle degree, and hence SOC is advanced at higher speeds to compensate for this effect. All three cylinders follow a similar trend. The deviation of combustion duration for different speeds is shown in Fig. 5(d). It is observed that at moderate speeds, the combustion duration is slightly lower, but the duration of combustion is found to increase when there is a rise in the engine speed, and the same trend is followed for all three cylinders.

3.3.2. Effect of torque on combustion parameters

The variation of combustion parameters as a function of torque for all three cylinders is presented in Fig. 6.

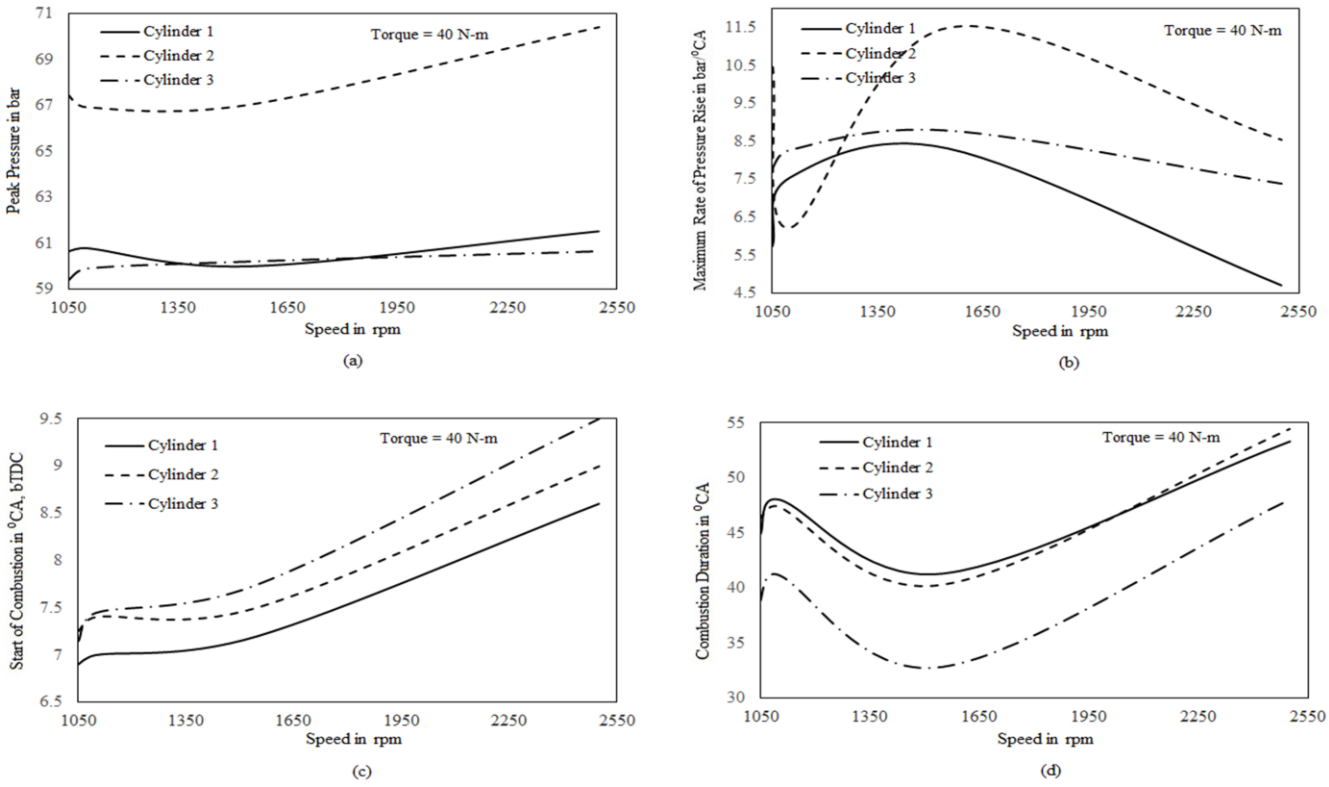

Fig. 5. Variation of combustion parameters with speed.

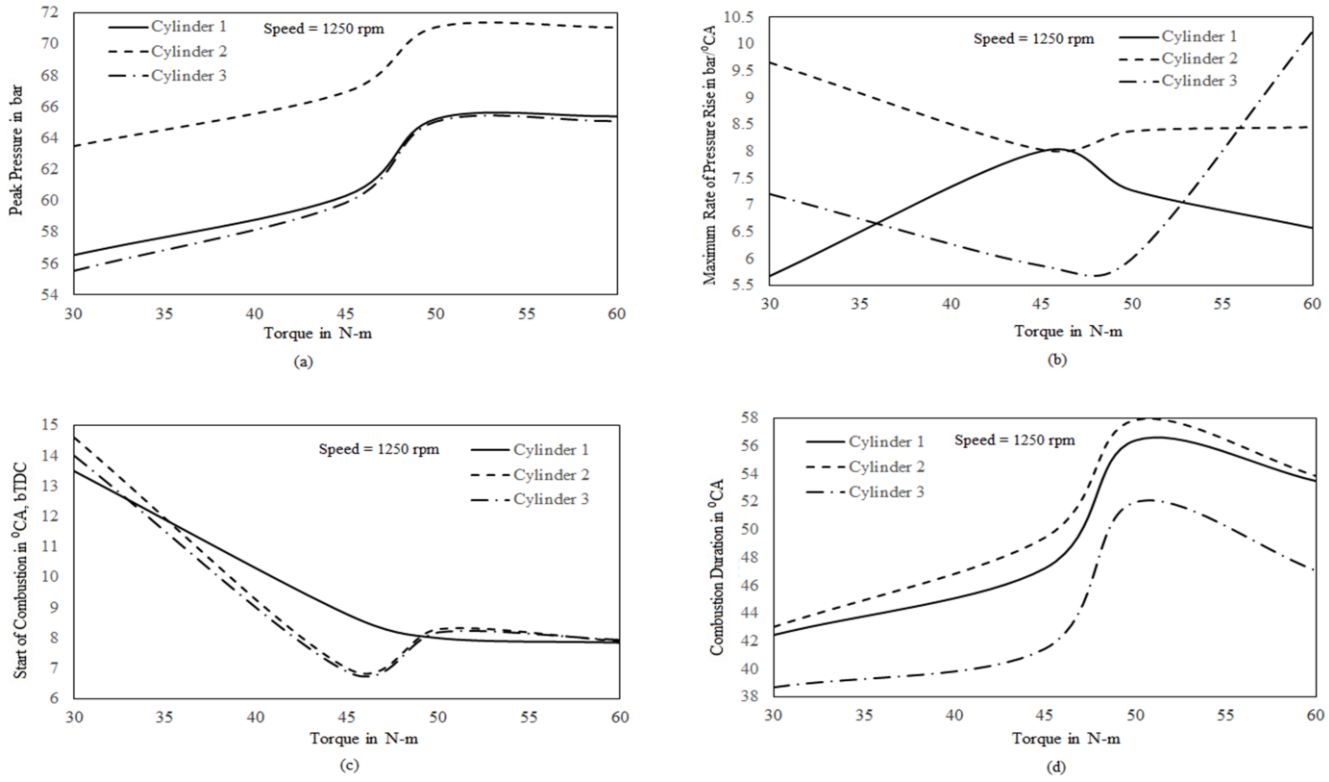

Fig. 6. Variation of combustion parameters with torque.

It was observed from Fig. 6(a) that the peak pressure of all three cylinders varies considerably when the engine is operated at various torques by maintaining a constant speed. As the torque is increased, the cylinder peak pressure also increases due to increased fuel burning at a higher torque, and a similar trend is found for all cylinders. Also, a similar trend of variation is ob-

served for the variation of peak pressure for the cylinders as reported in Fig. 5(a).

Figure 6(b) displays the manner in which the maximum rate of pressure rise varies as a function of torque. From the figure, it is clear that the variation between the cylinders shows an erratic trend. Figure 6(c) presents the fashion in which the start of combustion varies as a function of torque. It can be seen that the start of combustion is advanced as the engine is operated at higher torque values. This may be due to the enhanced fuel vaporisation at higher torques, and hence, an earlier start of combustion. Figure 6(d) shows the manner in which the combustion duration varies with respect to torque. An increasing trend is observed in the combustion duration for increased torque values, and all cylinders follow a similar trend. This is primarily because of the increased volume of charge burned as the torque increases.

3.3.3. Effect of speed and torque on maximum heat release rate

Variation of the maximum heat release rate resulting from fuel combusted through the duration of pilot injection and main injection as a function of speed is shown in Fig. 7.

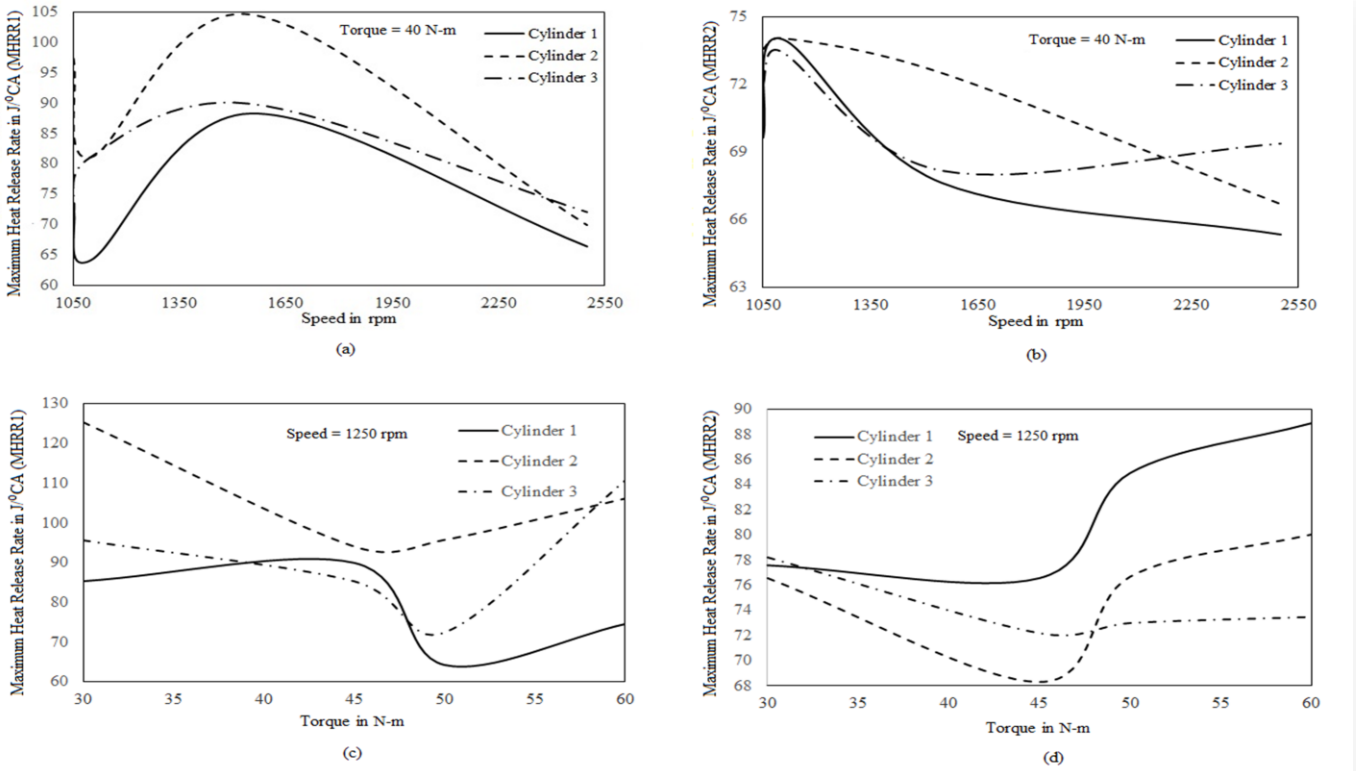

Fig. 7. Variation of MHRR1 and MHRR2 with speed and torque.

It is observed from Fig. 7(a) that an increase in speed leads to a rise in the value of MHRR1 initially, and further increasing the speed causes a decrease in MHRR1. At higher speeds, the duration of pilot injection will be short, and resulting in a lower MHRR1 when compared to MHRR1 recorded at lower speeds, and a similar trend is charted for all cylinders. Figure 7(b) shows that MHRR2 seems to be higher at lower speeds and tends to decrease slightly for higher speeds.

It is also observed in Fig. 7(c) that an increase in torque increases MHRR1 because of burning a higher fuel quantity at an increased torque. Figure 7(d) depicts that as the torque increases, MHRR2 resulting from the main injection also increases owing to an increase in volume of fuel burned at an increased torque.

3.4. Performance and emission parameters as a function of BMEP

In this section, the variations of carbon monoxide (CO), unburnt hydrocarbon (UBHC), oxides of nitrogen (NO_x) and brake thermal efficiency (BTE) are presented as a function of BMEP as a trade-off curve between NO_x-CO, NO_x-UBHC and NO_x-BTE.

From Fig. 8, it can be predicted that an increase in BMEP results in an increased quantity of NO_x. The value of BMEP is increased by burning an additional quantity of fuel to compensate for the increase in load, which results in a higher temperature inside the combustion chamber. It is obvious that higher temperatures favour the NO_x formation inside the combustion chamber. The value of NO_x reaches a maximum and tends to reduce due to the non-availability of oxygen at a higher BMEP. It can also be predicted that at a slightly increased BMEP, the quantity of UBHC and CO increases, because of overfuelling, a small portion of fuel remains unburned, and decreases as the combustion temperature is increased further. At a higher BMEP, due to an increased crevice volume and reduced quantity of oxygen, the amount of UBHC and CO will increase. A similar trend of variation is observed for BTE as for CO and UBHC. As BMEP increases, a slight reduction in BTE is observed at the

middle range of BMEP, and a further increase in BMEP results in an increasing trend for BTE with BMEP. This may be due to the increase in fuel consumption with torque. A decrease in BTE with BMEP during the middle range of BMEP may be due to the change in the engine speed when compared to that for the lower BMEP.

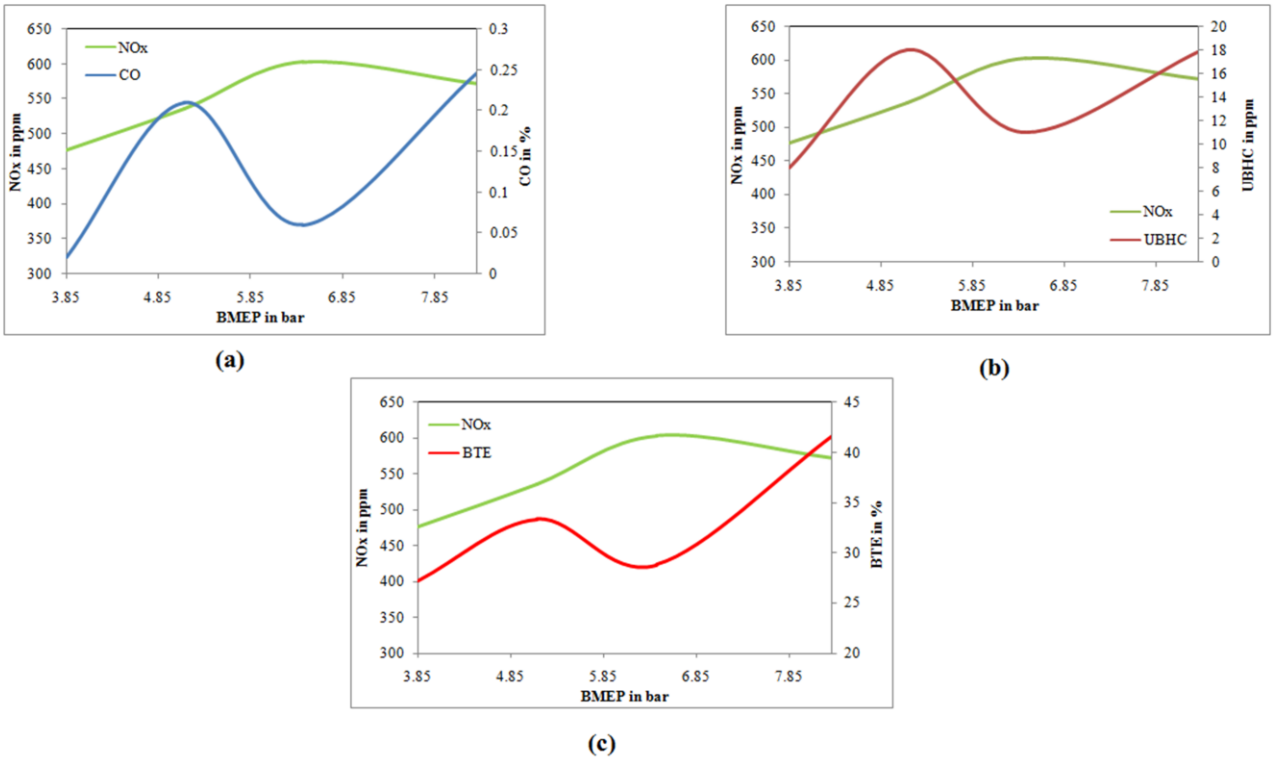

Fig. 8. Variation of performance and emission parameters with BMEP.

A trade-off between NO_x-CO, NO_x-UBHC and NO_x-BTE is observed at a higher BMEP close to 8 bar, where the two curves intersect each other. This point may be considered as an optimised condition for both the parameters presented in the graph. It is also observed that NO_x-UBHC and NO_x-CO curves intersect during the middle range of operation too, which indicates the operating condition for simultaneous control of NO_x, UBHC and CO emissions.

4. Conclusions

In the present work, performance and emission parameters and cylinder-to-cylinder variation of combustion parameters of a medium duty 3-cylinder CRDI passenger car diesel engine were investigated by testing the engine at different operating conditions. The following conclusions were made based on the findings:

- The combustion parameters vary considerably between the cylinders.
- The combustion parameters of cylinder 2 differ considerably from those of the other two cylinders. Its uncontrolled and controlled phase of combustion differs noticeably from those of the other two cylinders.
- The consistently elevated in-cylinder pressure in cylinder 2 was primarily attributed to a slight advance in the start of injection, resulting in earlier combustion and a higher peak pressure, as well as an increase in cumulative heat release. Minor compression differences, likely caused by carbon deposits on the piston crown, were also observed but considered secondary contributors.
- The extended combustion duration in cylinder 2 may be attributed to factors such as uneven air-fuel mixture distribution, variations in injector flow rate or spray pattern, and thermal variations between the cylinders. These factors, while not directly measured in this study, require further examination, recommended to identify the root cause of the observed asymmetry.
- The maximum heat release rate, maximum rate of pressure rise and cycle peak pressure for cylinder 2 were higher when compared with the other two cylinders.
- Cylinder 2 shows a marginally longer CD than the other cylinders.
- A trade-off point was obtained at a higher BMEP for simultaneous control of NO_x, CO and UBHC at a higher brake thermal efficiency.
- During the engine operation at a medium BMEP, it is possible to simultaneously control the NO_x, CO and UBHC emissions.

From this investigation, it can be concluded that a significant variation in the magnitude of combustion parameters was observed between the three cylinders of a passenger car engine. It can also be concluded that the engine emissions can be simultaneously controlled.

This work can be further extended to investigate the influence of biodiesel and higher alcohols on the performance, combustion and emission characteristics of the test engine, and the results can be compared with those of diesel. To maintain the combustion uniformity in CRDI engines, regular injector flow calibration and matching are recommended. A theoretical model can be developed, and the simulated results can be validated with the experimental results.

References

[1] Hyönen, J., Haraldsson, G., & Johansson, B. (2004). Balancing Cylinder-to-Cylinder Variations in a Multi-Cylinder VCR-HCCI Engine. *SAE Technical Paper 2004-0-1897*. doi: 10.4271/2004-01-1897

[2] Ohtsubo, H., Yamauchi, K., Nakazono, T., Yamane, K., & Kawasaki, K. (2007). Influence of Compression Ratio on Performance and Variations in Each Cylinder of Multi Cylinder Natural Gas Engine with PCCI Combustion. *SAE Technical Paper 2007-01-1877*. doi: 10.4271/2007-01-1877

[3] Johansson, B., & Einewall, P. (2000). Cylinder to Cylinder and Cycle to Cycle Variations in a Six Cylinder Lean Burn Natural Gas Engine. *SAE Technical Paper 2000-01-1941*. doi: 10.4271/2000-01-1941

[4] Stumpp, G., & Ricco, M.(1996). Common Rail – An Attractive Fuel Injection System for Passenger Car DI Diesel Engines. *SAE Technical Paper 960870.* doi: 10.4271/960870

[5] Guerrassi, N., & Dupraz, P.(1998). A Common Rail Injection System For High Speed Direct Injection Diesel Engines. *SAE Technical Paper 980803*. doi: 10.4271/980803

[6] Torregrosa, A., Broatch, A., Garcá, A., & Mónico, L. (2013). Sensitivity of combustion noise and NO_x and soot emissions to pilot injection in PCCI diesel engines. *Applied Energy,* 104, 149−157. doi: 10.1016/j.apenergy.2012.11.040

[7] Huang, H., Liu, Q., Yang, R., Zhu, T., Zhao, R., & Wang, Y. (2015). Investigation on the effects of pilot injection on low temperature combustion in high-speed diesel engine fueled with n-butanol–diesel blends. *Energy Conversion and Management,*106, 748−758. doi: 10.1016/j.enconman.2015.10.031

[8] Barsic, N., & Humke, A.L. (1981). Performance and Emissions Characteristics of a naturally aspirated diesel engine with vegetable oil fuels. *Transaction of SAE, Technical Paper 810262,* doi: 10.4271/810262

[9] Hemmerlein, N., Korte, V., Richter, H., & Schröeder, G. (1991). Performance, Exhaust Emissions and Durability of Modern Diesel Engines Running on Rapeseed Oil. *Transaction of SAE, Technical Paper 910848.* doi: 10.4271/910848.

[10] Huang, H., Zhou, C., Liu, Q., Wang, Q., & Wang, X. (2016). An experimental study on the combustion and emission characteristics of a diesel engine under low temperature combustion of diesel/gasoline/n-butanol blends. *Applied Energy*, 170, 219−231. doi: 10.1016/j.apenergy.2016.02.126

[11] Saravanan, S., Nagarajan, G., & Lakshmi Narayana, R.G. (2009). Comparison of Combustion Characteristics of Crude Rice Bran Oil Methyl Ester with Diesel as a CI Engine Fuel. *Journal of Biobased Materials and Bioenergy*, 3, 32−36. doi: 10.1166/jbmb.2009.1003

[12] Singh, A.K., Palia, H.S., & Khan, M.M. (2024). Experimental investigations of CI engine performance using ternary blends of n-butanol/biodiesel/diesel and n-octanol/biodiesel/diesel, *Archives of Thermodynamics*, 45, 109−118. doi: 10.24425/ather.2024.150443

[13] Kumara, D., Kumar, N., & Chaudhary, R. (2024). Use of butanol, pentanol and diesel in a compression ignition engine: A review, *Archives of Thermodynamics*, 45, 27−35. doi: 10.24425/ather.2024.151994

[14] Kollol, A. Reddy, N., Paruvada, S., & Murugan, S. (2019). Experimental studies of a diesel engine run on biodiesel n-butanol blends. *Renewable Energy*, 135, 687−700. doi: 10.1016/j.renene.2018.12.011

[15] Sayon, S., Joel, B., Tizane, D., Gilles, V., & Jean, K. (2020). Comparative study of three ways of using Jatropha curcas vegetable oil in a direct injection diesel engine. *Scientific African*, 7, e00290. doi: 10.1016/j.sciaf.2020.e00290

[16] Canakci, M., Ozsazen, A.N., & Turkcan, A. (2009). Combustion analysis of preheated crude sunflower oil in an IDI diesel engine. *Biomass and Bioenergy*, 33(5), 760−767. doi: 10.1016/j.biombioe.2008.11.003

[17] Kandasamy, S.K., Selvaraj, A.S., & Rajagopal, T.K.R. (2019). Experimental investigations of ethanol blended biodiesel fuel on automotive diesel engine performance, emission and durability characteristics. *Renewable Energy*, 141, 411−419. doi: 10.1016/j.renene.2019.04.039

[18] Qi, D.H., Lee, C.F., Jia, C.C., Wang, P.P., & Wu, S.T. (2014). Experimental investigations of combustion and emission characteristics of rapeseed oil–diesel blends in a two cylinder agricultural diesel engine. *Energy Conversion and Management*, 77, 227−232. doi: 10.1016/j.enconman.2013.09.023

[19] Ali, O.M., Mamat, R., Abdullah, N.R., & Abdullah, A.A. (2016). Analysis of blended fuel properties and engine performance with palm biodiesel–diesel blended fuel. *Renewable Energy*, 86, 59−67. doi: 10.1016/j.renene.2015.07.103

[20] Jayaprabakar, J., Karthikeyan, A., & Rameshkumar, V. (2017). Effect of injection timing on the combustion characteristics of rice bran and algae biodiesel blends in a compression-ignition engine. *International Journal of Ambient Energy*, 38, 116−121. doi: 10.1080/01430750.2015.1048901

[21] Rama Krishna Reddy, E., Subbalakshmi, Y., Dhana Raju, V., Appa Rao, K., Harun Kumar, M., Rami Reddy, S., & Tharun Sai, P. (2019). Assessment of performance, combustion and emission characteristics of the diesel engine powered with corn biodiesel blends. *International Journal of Ambient Energy*, 40, 435−443. doi: 10.1080/01430750.2019.1636867

[22] Ganesan, S., Devaraj, A., & Devarajan, Y. (2020). Emission characteristics on single cylinder diesel engine using biofuels. *International Journal of Ambient Energy*, 41, 1613−1616. doi: 10.1080/01430750.2018.1517694

[23] Jindal, S., Nandwana, B.P., Rathore, N.S., & Vashistha, V. (2010). Experimental investigation of the effect of compression ratio and injection pressure in a direct injection diesel engine running on Jatropha methyl ester. *Applied Thermal Engineering*, 30(5), 442−448. doi: 10.1016/j.applthermaleng.2009.10.004

[24] Pradeep, V., & Sharma, R.P. (2005). Evaluation of Performance, Emission and Combustion Parameters of a CI Engine Fuelled with Bio-Diesel from Rubber Seed Oil and its Blends. *Transactions of SAE, Technical Paper 2005-26-353*. doi: 10.4271/2005-26-353

[25] Ganapathy, T., Gakkhar, R.P., & Murugesan, K. (2011). Influence of injection timing on performance, combustion and emission characteristics of Jatropha biodiesel engine. *Applied Energy*, 88, 4376−4386. doi: 10.1016/j.apenergy.2011.05.016

[26] Hirkude, J.B., & Padalkar, A.S. (2014). Performance optimization of CI engine fuelled with waste fried oil methyl ester-diesel blend using response surface methodology. *Fuel*, 119, 266−273. doi: 10.1016/j.fuel.2013.11.039

[27] Bari, S., Yu, C.W., & Lim, T.H. (2004). Effect of fuel injection timing with waste cooking oil as a fuel in a direct injection diesel engine. *Proceedings of the Institution of Mechanical Engineers; part D, Journal of Automobile Engineering*, 18, 93−104. doi: 10.1243/095440704322829209

[28] Agarwal, A.K., Srivastava, D.K., Dhar, A., Maurya, R.K., Shukla, P.C., & Singh, A.P. (2013). Effect of fuel injection timing and pressure on combustion, emissions and performance characteristics of a single cylinder diesel engine. *Fuel*, 111, 374−383. doi: 10.1016/j.fuel.2013.03.016

[29] Payri, F., Benajes, J., Arrègle, J., & Riesco, J.M. (2006). Combustion and Exhaust Emissions in a Heavy-Duty Diesel Engine with Increased Premixed Combustion Phase by Means of Injection Retarding. *Oil & Gas Science and Technology – Rev. IFP*, 61(2), 247−258. doi: 10.2516/ogst:2006018x

[30] Tauzia, X., Maiboom, A., & Shah, S.R. (2010). Experimental study of inlet manifold water injection on combustion and emissions of an automotive direct injection diesel engine. *Energy*, 35, 3628−3639. doi: 10.1016/j.energy.2010.05.007

[31] Saravanan, S., Nagarajan, G., & Lakshmi Narayana, R.G. (2009). Feasibility analysis of crude rice bran oil methyl ester blend as a stationary and automotive diesel engine fuel. *Energy for Sustainable Development*, 13(1), 52−55. doi: 10.1016/j.esd.2009.03.001

[32] Saravanan, S., Nagarajan, G., & Sampath, S. (2011). Investigation on combustion characteristics of crude rice bran oil methyl ester blend as a heavy duty automotive engine fuel. *International Journal of Oil, Gas and Coal Technology*, 4(3), 282−295. doi: 10.1504/IJOGCT.2011.040840

[33] Sidibe, S., Blin, J., Daho, T., Vaitilingom, G., & Koulidiati, J. (2020). Comparative study of three ways of using Jatropha curcas vegetable oil in a direct injection diesel engine, *Scientific African*, 7, e00290. doi: 10.1016/j.sciaf.2020.e00290

[34] Kandasamy, S.K., Selvaraj, A.R., & Rajagopal, T.K.R. (2019). Experimental investigations of ethanol blended biodiesel fuel on automotive diesel engine performance, emission and durability characteristics, *Renewable Energy*, 141, 411−419. doi: 10.1016/j.renene.2019.04.039

[35] Devarajan, Y., Munuswamy, D., Nagappan, B., & Subbiah, G. (2019). Experimental assessment of performance and exhaust emission characteristics of a diesel engine fuelled with Punnai biodiesel/butanol fuel blends, *Petroleum Science*, 16, 1471−1478. doi: 10.1007/s12182-019-00361-9

[36] Roy, S., Banerjee, R., Das, A.K., & Bose, P.K. (2014). Development of an ANN based system identification tool to estimate the performance-emission characteristics of a CRDI assisted CNG dual fuel diesel engine. *Journal of Natural Gas Science and Engineering*, 21, 147−158. doi: 10.1016/j.jngse.2014.08.002

[37] Roy, S., Ghosh, A., Das, A.K, & Banerjee, R. (2014). A comparative study of GEP and an ANN strategy to model engine performance and emission characteristics of a CRDI assisted single cylinder diesel engine under CNG dual-fuel operation. *Journal of Natural Gas Science and Engineering*, 21, 814−821. doi: 10.1016/j.jngse.2014.10.024

[38] Hwang, J., Qi, D., Jung, Y., & Bae, C. (2014). Effect of injection parameters on the combustion and emission characteristics in a common-rail direct injection diesel engine fueled with waste cooking oil biodiesel. *Renewable Energy*, 63, 9−17. doi: 10.1016/j.renene.2013.08.051

[39] Syed Aalam, C., Saravanan, C.G., & Kannan, M. (2015). Experimental investigations on a CRDI system assisted diesel engine fuelled with aluminium oxide nanoparticles blended biodiesel. *Alexandria Engineering Journal*, 54, 351−358. doi: 10.1016/j.aej.2015.04.009

[40] Basavarajappa, D.N., Banapurmath, N.R., Khandal, S.V., & Manavendra, G. (2015). Performance Evaluation of Common Rail Direct Injection (CRDI) Engine Fuelled with Uppage Oil Methyl Ester (UOME), *International Journal of Renewable Energy Development*, 4(1), 1−10. doi: 10.14710/ijred.4.1.1-10

[41] Ashok, B., Nanthagopal, K., Chaturvedi, B., Sharma, S., & Thundil Karuppa Raj, R. (2018). A comparative assessment on Common Rail Direct Injection (CRDI) engine characteristics using low viscous biofuel blends, *Applied Thermal Engineering*, 145, 494−506. doi: 10.1016/j.applthermaleng.2018.09.069

[42] Choi, B., Kim, Y.K., Jung, G., Lee, C., Jiang, X., & Choi, I. (2014). Effect of Diesel Fuel Blend with Biobutanol on the Emission of Turbocharged CRDI Diesel Engine. *Energy Procedia*, 61, 2145−2148. doi: 10.1016/J.EGYPRO.2014.12.096

[43] Choi, B., & Jiang, X. (2015). Individual hydrocarbons and particulate matter emission from a turbocharged CRDI diesel engine fuelled with n-butanol/diesel blends. *Fuel*, 154, 188−195. doi: 10.1016/J.FUEL.2015.03.084

[44] Babu, J.M., Prasad, K.S., Ganji, P.R., Ravikiran, Ch., & Velu, R. (2022). Analysis on the effect of pilot injection strategies on combustion and emission characteristics of palm-munja biodiesel/diesel blend on CRDI diesel engine. *International Journal of Ambient Energy*, 43(1), 618−621. doi: 10.1080/01430750.2019.1663368

[45] Senthil Kumar, D., & Thirumalini, S. (2022). Effect of injection parameters and EGR on performance and emissions in a CRDI engine fuelled with cashew nut shell biodiesel blend. *International Journal of Ambient Energy*, 43, 3085−3095. doi: 10.1080/01430750.2020.1796786

[46] Saravanan, S., Durai, K.P., & Sundaram, I.M. (2019). Comparison of combustion characteristics of an automotive CRDI engine with conventional HCV engine. *International Journal Oil, Gas and Coal Technology*, 21(3), 390−405. doi: 10.1504/IJOGCT.2019.10021964

[47] Moffat, R.J. (1985). Using uncertainty analysis in the planning of an experiment. *Transaction of ASME, Journal Fluids Engineering*, 107(2), 173−178.